Surface-Controlled Electroless Deposition Method in the Preparation of Stacked Silver Nanoparticles on Germanium for Surface-Enhanced Infrared Absorption Measurements

RUO-LAN JOAN CHANG and JYISY YANG*

Department of Chemistry, National Chung-Hsing University, Taichung 402, Taiwan

A new method to prepare highly sensitive sensing elements for surface-enhanced infrared absorption (SEIRA) measurements was investigated. A surface-controlled procedure was employed to grow round and stacked silver nanoparticles (Ag-NPs) on germanium substrates. In this method, an initial layer of Ag-NPs was prepared using a common method of electroless deposition. After subsequently placing a controlled layer of *p*-aminothiophenol (*p*ATP) on the surface of the initial layer of Ag-NPs, the substrates were placed in a silver nitrate solution to grow a second layer of Ag-NPs. By repeating these growing procedures, multi-layers of stacked Ag-NPs can be obtained. To examine the influence of morphology of the formed Ag-NPs on the resulting SEIRA signals, the factors affecting the reactions were systematically examined. These factors included the concentrations of silver nitrates, the reaction times to prepare both the initial layer and the second layer of Ag-NPs, and the coverage of *p*ATP. Results indicate that the Ag-NPs making up the second layer were round in shape and much more densely distributed than those in the initial layer. The observed SEIRA spectra did not show derivative-shaped absorption bands for *p*ATP on the Ag-NPs after re-growth, indicating that *p*ATP was sandwiched between the two layers of Ag-NPs, preventing the nanoparticles from coming into direct contact with one another. Also, the SEIRA signals of the controlled molecules between the particles were found to be two to five times more intense than the signals before growing another layer of Ag-NPs. The reaction conditions can be adjusted to vary the morphology and thickness of the Ag-NP layers, and, by repeating the growing procedures, a thick layer of stacked Ag-NPs with suitable size for SEIRA measurements can be obtained that is highly suited to chemical sensing applications.

Index Headings: **Surface-enhanced infrared absorption spectroscopy; SEIRAS; Silver nanoparticles; Ag-NPs; Electroless deposition.**

INTRODUCTION

Since the first report of the phenomenon of surface-enhanced infrared absorption spectroscopy,[1] it has attracted considerable attention because of its potential as a sensitive analysis tool in widespread applications. Surface-enhanced infrared absorption (SEIRA) relies on the localized electric fields around metallic nanoparticles (NPs) that enhance the dipole moments of the adsorbed molecules of NPs and hence the absorptions of the adsorbed molecules. In general, the enhancement factor depends on the chemical nature of the adsorbed species, the size and morphology of the NPs,[2,3] the attributes of the metals,[4–6] and the materials used as substrates.[5,7,8] According to the literature, large enhancement factors have been observed when the thickness of metal films is limited to 4 to 10 nm, with the diameter of the NPs around three times the thickness of the metal films.[5,8–10] Once the metals are percolated, the absorption bands are distorted to derivative band shapes.[5,11] Metals vary in their enhancement capabilities. Specifically, Ag,[1,3,5,6,8–10,12–17] Au,[12,15–17] Pt,[4,6,18] Cu,[13,15,17] In,[17] Sn,[19] Zn,[5] and others[4,20–22] have been shown to provide enhancement factors varying from one to three orders of magnitude, with the level of enhancement depending on the metal used and the morphology of the nanoparticles.

To prepare active substrates, the vapor deposition method (PVD) is the most commonly used method for SEIRA measurements.[1,5,16,19,23,24] This method produces NPs with prolate-ellipsoid shapes, the sizes of which are controlled mainly by the physical deposition conditions.[5,16,19,23,24] However, this method has several weaknesses. For instance, significant operational skill is required to achieve reproducibility in the preparation of the metal films. Also, the range of sizes and shapes of the metal island are generally quite limited, and the method is applicable only to flat substrates. To address these issues, electroless deposition methods for SEIRA measurements have been developed, such as production of Ag-NPs on polymeric substrates,[25] or deposition of metallic nanoparticles on germanium[11,26,27] and silicon substrates.[28–38] With electroless deposition, the enhancement factor is about two orders of magnitude for NPs approximately 100 nm in diameter.[11] This method is simple, low in cost, highly reproducible, and effective in preparing metallic NPs on both flat and non-flat substrates. Also, it offers the potential of controlling the morphologies of the NPs by varying the reaction conditions.

In this study, an electroless deposition method was used to prepare stacked Ag-NPs for the potential application of SEIRA in chemical sensing. To prepare stacked NPs with properties similar to those of isolated NPs, a thin layer of organic substance on the surface of an initial layer of isolated Ag-NPs is proposed to control the growth of an additional layer of Ag-NPs. This organic substance is used to coat most of the surface of the base-layer Ag-NPs, thus allowing only a limited area for additional growth of Ag-NPs. Figure 1 illustrates the concept to produce stacked but isolated Ag-NPs. In these procedures, Ag-NPs were first grown on Ge substrates by soaking the substrate in a solution containing an appropriate concentration of silver ions to form the desired size of Ag-NPs. After preparing the first layer of Ag-NPs, a thin layer of organic compound was placed on the surface of the Ag-NPs to block most of the surface area; *p*-aminothiophenol (*p*ATP) was used as the organic compound in this work due to its low solubility in aqueous solutions and its ease of forming a monolayer. When the substrate was again placed in the silver reaction solution, further growth of Ag-NPs was restricted to the unblocked surface of the Ag-NPs under the condition that the reducing electrons from the Ge substrates favor passing through the Ag-NPs to the silver ions. To simplify the system for description, the first layer of Ag-NPs is notated A^PAg, representing growth of A minutes in P mM of silver nitrate; after the placement of

Received 17 July 2009; accepted 3 December 2009.
* Author to whom correspondence should be sent. E-mail: jyisy@dragon.nchu.edu.tw.

0003-7028/10/6402-0211$2.00/0

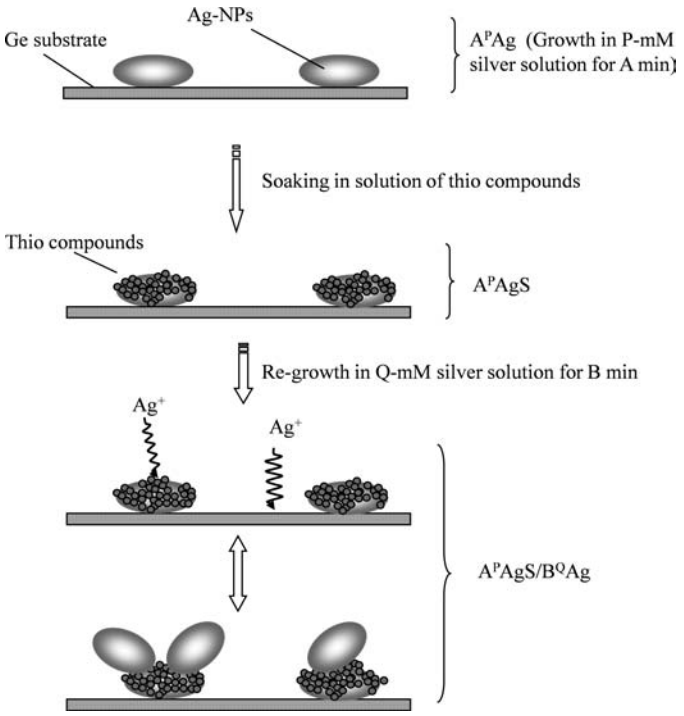

FIG. 1. Schematic diagram of re-growing silver nanoparticles on Ag-NPs/Ge by the surface modification method.

the organic (thio) blocking compound, the notation becomes A^PAgS. With the addition of the second layer of Ag-NPs, the notation is A^PAgS/B^QAg for re-growing of B minutes in Q mM of silver nitrate; for a third layer of Ag-NPs, it is notated A^PAgS/B^QAgS/C^RAg for re-growing of the A^PAgS/B^QAgS for C minutes in R mM of silver nitrate solution.

The success of the above-proposed procedure in producing stacked Ag-NPs relies on the assumption that the electrons from the Ge preferentially pass through Ag-NPs to silver ions. If the efficiency of transferring electrons directly from the Ge to the silver ions were sufficiently high, the re-soaking of the Ge substrate in the silver solution would cause significant percolation, as all the residual surfaces of the Ge would be in direct contact with the silver ions. Fortunately, the reduction process involves the electron passing through the silver atoms, rather than moving directly from the Ge to the silver ions, as the reduced silver atoms tend to coagulate to a size of 100 nm in diameter as observed in our previous study.[11]

To investigate the feasibility of this proposed method of growing stacked Ag-NPs on Ge substrates for SEIRA measurements, factors such as the concentration of silver ions, the reaction time for both the initial and the additional layer of Ag-NPs, and the coverage of the thio compounds on the first layer of Ag-NPs were examined with regard to their influence on the enhanced IR signals and Ag-NP morphologies.

MATERIALS AND METHODS

Reagent. Silver nitrate was purchased from Pro-Chem (Rockford, IL). Methanol was purchased from Echo Chemical Co. (Toufen, Taiwan). The probe molecule, *p*-aminothiophenol (*p*ATP), was purchased from Aldrich (Milwaukee, WI) and used as received. N-type germanium disks were purchased from Lattice Materials Co. (Bozeman, MT). These disks were 0.5 inches in diameter and 4 mm in thickness. The resistivities

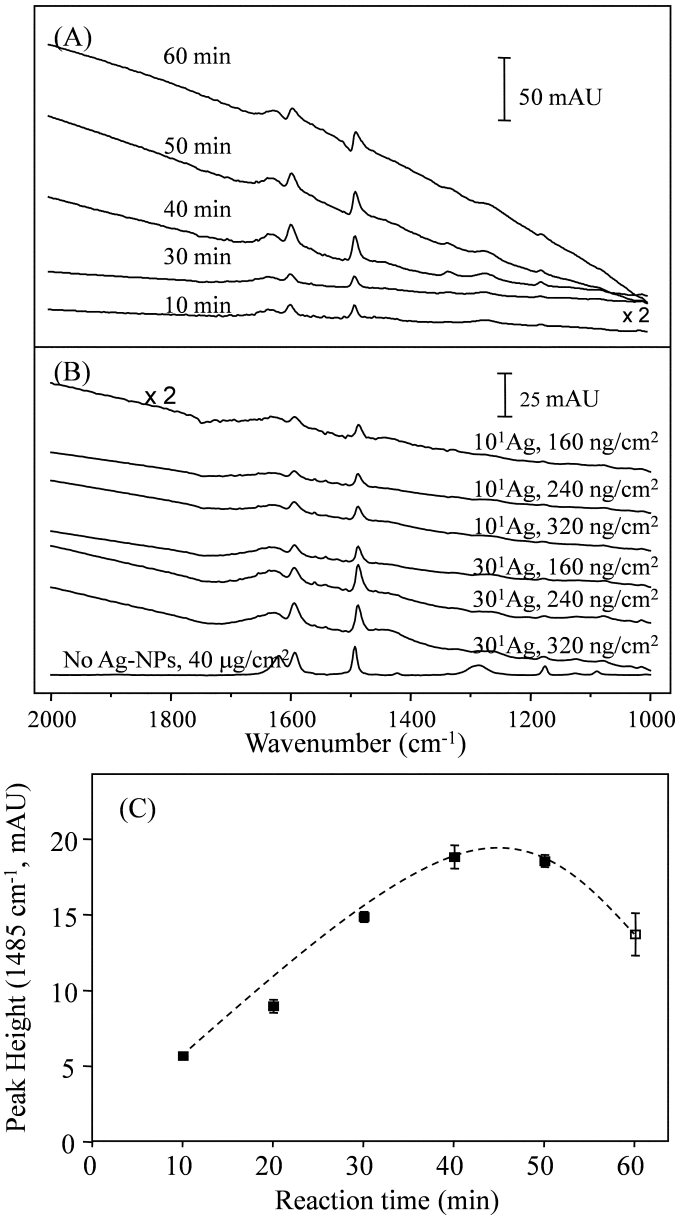

FIG. 2. (**A**) Typical SEIRA spectra of *p*ATP on Ag-NPs/Ge prepared by soaking in 1 mM $AgNO_3$ for different times at 4 °C. Ag-NPs/Ge substrates were soaked in 10 mg/L *p*ATP solution overnight. (**B**) *p*ATP deposited on bare Ge, 10^1Ag, and 30^1Ag. The surface density of *p*ATP on bare Ge was 40 μg/cm^2 and the amounts of *p*ATP on 10^1Ag and 30^1Ag were 320, 240, and 160 ng/cm^2. (**C**) Band intensities of *p*ATP on Ag-NPs/Ge substrates. Substrates of Ag-NPs/Ge were prepared by immersing in 1 mM $AgNO_3$ for different reaction times. Distortion of the band shape was observed as labeled by the open symbols.

of the Ge disks were 4 to 50 Ω/cm and their purities were higher than 99.999%. Aluminum oxide purchased from Leco Co. (Joseph, MI) with a diameter of 0.05 μm was used for polishing the Ge substrates.

Preparation of Silver Nanoparticles on Germanium. The Ge substrates were polished (aluminum oxide, 0.05 μm), cleaned (deionized water), and dried (80 °C for 20 minutes). After being removed from the oven and rinsed with deionized water for 2 minutes, the Ge substrates were immersed in a silver nitrate solution for a series of different reaction times. The reaction temperature was controlled by an ice-water bath; at the end of the designated reaction time, the Ge substrates

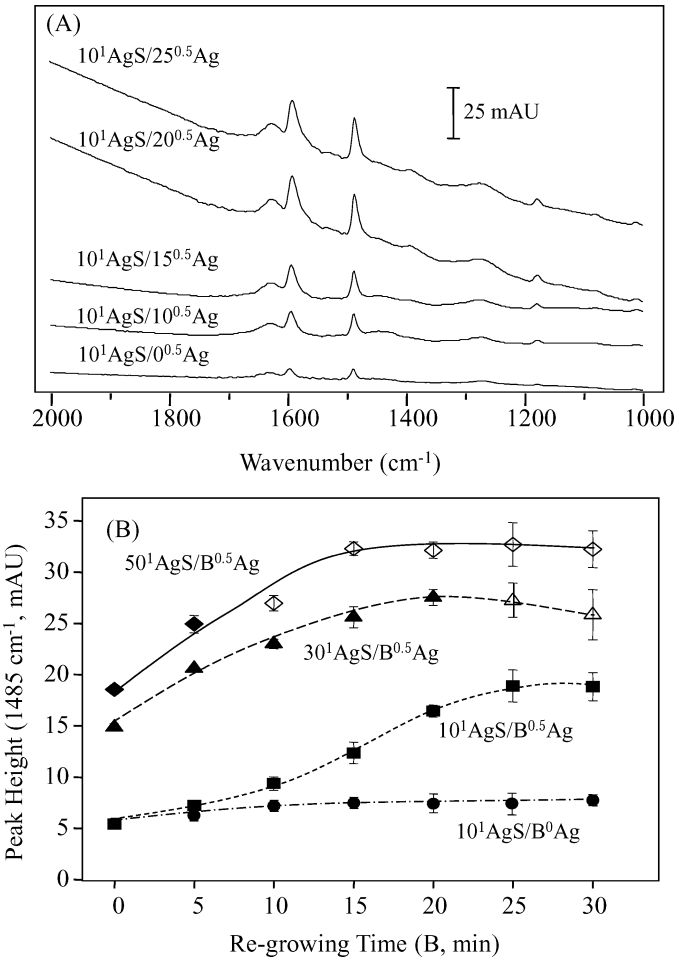

FIG. 3. (**A**) Spectra of *p*ATP of 10^1AgS/$B^{0.5}$Ag substrates, where $B = 0$, 10, 15, 20, and 25 minutes. (**B**) Band intensities of *p*ATP on substrates of 10^1AgS (■), 30^1AgS (▲), and 50^1AgS (♦) after re-growing in 0.5 mM silver nitrate solution for different lengths of time. Band intensities of *p*ATP on 10^1AgS (●) after soaking in water for different lengths of time are also plotted. Distortion of the band shape was observed as labeled by the open symbols.

were removed from the silver nitrate solution and soaked in deionized water for 5 minutes to terminate the reaction. The substrates were then rinsed in methanol and placed in a 10 mg/L solution of *p*ATP for designated times to effect varying degrees of coverage of chemisorbed layers of *p*ATP.

Procedures for Re-growing of Silver Nanoparticles. After the surface of the initial layer of Ag-NPs was treated with *p*ATP, the substrates were placed into prepared solutions of silver nitrate and the reaction temperature was controlled by ice-water bath. The concentration of silver nitrates and reaction times were varied to examine the factors influencing the growth of a second layer of Ag-NPs. At the end of the reaction, these substrates were removed from the reaction vessel and rinsed in deionized water for 5 minutes to stop the reaction. After then being rinsed with methanol and air dried, transmission infrared spectra were acquired by FT-IR spectrometry, using a Tensor 27 (Bruker Optics, Ettlingen, Germany) equipped with a deuterated triglycine sulfate (DTGS) detector. Data were acquired to 4 cm^{-1} resolution by co-adding 24 scans for each sample. Background spectra were collected using a bare Ge substrate.

RESULTS AND DISCUSSION

Basic Properties of the First Layer of Silver Nanoparticles in Detecting *p*-Aminothiophenol. To provide a basis for comparison, the Ag-NPs were first grown on a Ge substrate in a 1 mM solution of silver nitrate for different reaction times. The reaction temperature was controlled by ice-water bath. After soaking these prepared substrates in *p*ATP solution overnight, transmission spectra were acquired and the typical observed spectra are plotted in Fig. 2A. As can be seen, band intensities increased with reaction time, up to approximately 40 minutes. With a reaction time longer than 50 minutes, derivative-shaped absorption bands are observed, which are the result of percolated Ag-NPs. To estimate the quantities of *p*ATP adsorbed on the surface of the Ag-NPs, depositions of different amounts of *p*ATP were made on substrates of 10^1Ag and 30^1Ag. The resulting spectra are plotted in Fig. 2B along with the neat spectrum of *p*ATP, which was prepared by depositing *p*ATP at a surface density of 40 μg/cm^2 on a Ge substrate. As can be seen from these spectra, the surface area of the 10^1Ag substrate is smaller than that of 30^1Ag, as the maximum signals for the former were observed for a deposition of 160 ng/cm^2, with no further increase in intensity even with larger quantities of *p*ATP. For the 30^1Ag substrate, the largest signal was observed at 300 ng/cm^2. These results reveal that the monolayer of *p*ATP formed by soaking approximated a surface density of 200 to 300 ng/cm^2. To quantitatively observe the relationship between enhanced signals and reaction time in the formation of Ag-NPs, the band intensities at 1485 cm^{-1} were calculated and are plotted in Fig. 2C. As can be seen in this figure, the maximal band intensity was located at a reaction time of 40 minutes. To estimate the surface-enhancement factor from the first layer of Ag-NPs, the intensities of the absorption bands at 1485 cm^{-1} for the enhanced spectrum and neat spectrum were compared and indicated an enhancement factor of 100.

Behavior in Re-growing of Silver Nanoparticles on Germanium Substrates. To examine the feasibility of preparing stacked Ag-NPs by a second reduction step after blocking surface sites, an initial layer of Ag-NPs was prepared by soaking the substrate in a 1 mM solution of silver nitrate for a reaction time of 10 minutes. These prepared 10^1Ag substrates were then further soaked in a 10 mg/L *p*ATP solution overnight, to form 10^1AgS substrates, with a monolayer of chemisorbed *p*ATP. These substrates were then placed into a 0.5 mM solution of silver nitrate to grow an additional layer of Ag-NPs, with the re-growing time systematically varied. After rinsing and air drying, IR spectra were acquired. The typical resulting spectra of the remaining *p*ATP are plotted in Fig. 3A, and the relationship between band intensities and re-growing time is plotted in Fig. 3B. The 10^1AgS substrates were also soaked in water to determine the impact on the *p*ATP signals; the subsequent variations of the signals of *p*ATP on 10^1AgS are plotted in Fig. 3B for reference (labeled as 10^1AgS/B^{0}Ag). As these figures show, the spectral features are similar to each other, but the presence of the second layer of Ag-NPs significantly increases the band intensities of the chemisorbed *p*ATP; with the second layer the signals increased from 5 mAU to 18 mAU. As also shown in Fig. 3B, re-soaking the Ag-NP substrates in water yielded no significant variations in the band intensities, indicating that the *p*ATP was firmly adsorbed on the Ag-NPs and that the morphologies of Ag-NPs remained the same despite exposure to water for a significant amount of

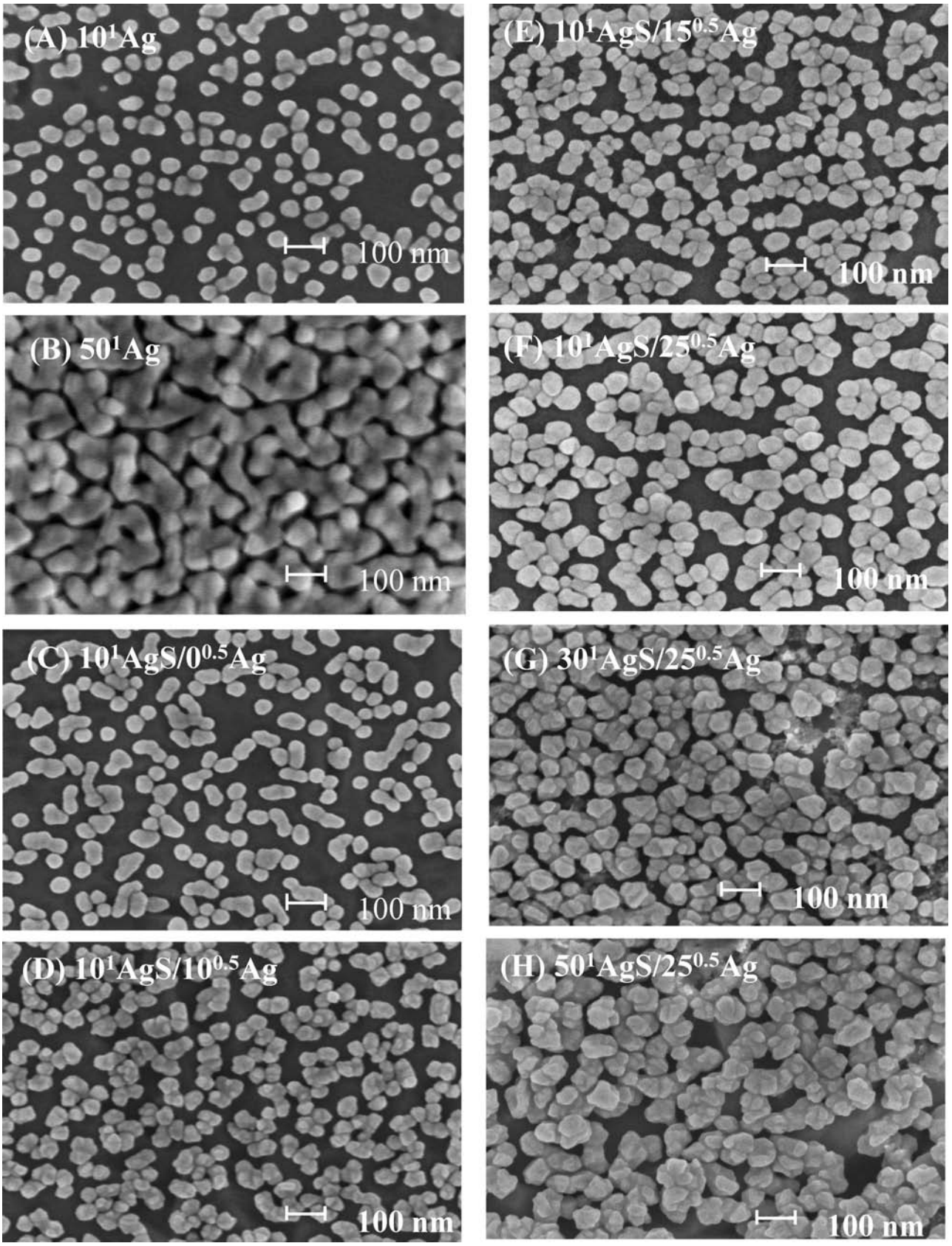

FIG. 4. SEM images of (**A**) 10^{1}Ag, (**B**) 50^{1}Ag, (**C**) 10^{1}AgS/$0^{0.5}$Ag, (**D**) 10^{1}AgS/$10^{0.5}$Ag, (**E**) 10^{1}AgS/$15^{0.5}$Ag, (**F**) 10^{1}AgS/$25^{0.5}$Ag, (**G**) 30^{1}AgS/$25^{0.5}$Ag, and (**H**) 50^{1}AgS/$25^{0.5}$Ag.

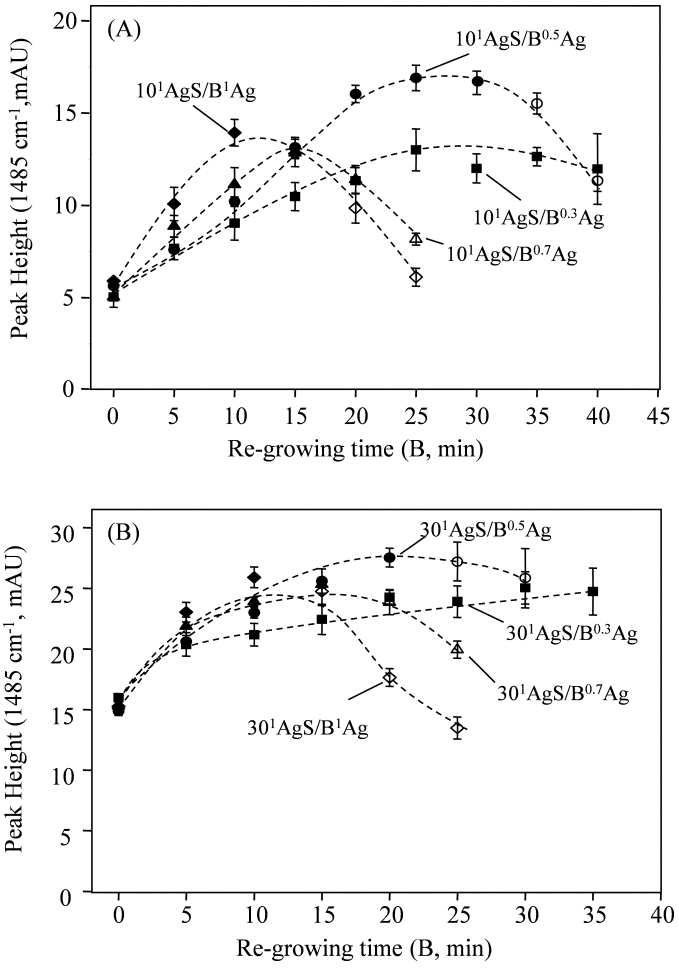

FIG. 5. (**A**) Band intensities of *p*ATP on substrates of 10^1AgS after re-growing in 0.3 (■), 0.5 (●), 0.7 (▲), and 1 mM (♦) silver nitrate solutions for different reaction times. Distortion of the band shape was observed as labeled by the open symbols. (**B**) Band intensities of *p*ATP on substrates of 30^1AgS after re-growing in 0.3 (■), 0.5 (●), 0.7 (▲), and 1 mM (♦) of silver nitrate solutions for different reaction times. Distortion of the band shape was observed as labeled by the open symbols.

time. This also indicated that the increase of the signal was caused by the increase of the enhancement factor for molecules between Ag-NPs, in the so-called "hot spots".

For comparisons in later analyses, the 10^1Ag and 50^1Ag substrates were imaged with a scanning electron microscope (SEM) and the resulting images are plotted in Figs. 4A to 4B. As can be seen in these figures, the diameter of the Ag-NPs on the 10^1Ag substrate is about 40 nm and as the reaction time increased, the particle size was increased to approximately 100 nm in diameter as shown in Fig. 4B. For the substrate of 50^1Ag, the degree of non-isolated Ag-NPs or the so-called degree of percolations was increased, as can be seen in Fig. 4B. To compare the morphologies of the Ag-NPs after re-growing in the silver nitrate solution, substrates of 10^1AgS, 10^1AgS/$10^{0.5}$Ag, 10^1AgS/$15^{0.5}$Ag, and 10^1AgS/$25^{0.5}$Ag were scanned using SEM; the resulting images are plotted in Figs. 4C through 4F. As can be seen in Fig. 4C, the 10^1AgS substrate, after the formation of a monolayer of *p*ATP, retained a morphology very similar to that of freshly prepared 10^1Ag (refer to Fig. 4A). After re-growing in silver nitrate solution, the resulting second layer of Ag-NPs was, as predicted, attached to the surface of the initial layer of Ag-NPs, forming a denser second layer. Also, as the re-growing time was increased, the particle size increased as well, as illustrated by the difference in size shown between Figs. 4D and 4F. In all cases, the Ag-NPs were consistently sized to one another and round in shape. The formation of the second layer of Ag-NPs directly on the top of the first layer of Ag-NPs could be caused by the blocking of the surface of Ge after soaking in *p*ATP solution to restrict the reduction of silver ions directly on the Ge substrate, or the electrons from Ge were given through the under layer of Ag-NPs to the silver ions in the solution. To clarify the growing mechanism, an attenuated total reflection crystal (ATR) of Ge (12 internal reflections) was soaked in *p*ATP solution over night. After air drying, infrared spectra were acquired by FT-IR spectrometry with modes of ATR and reflection-absorption (80 degree incident angle with a polarizer). However, no obvious spectral feature was observed, indicating that the interaction between Ge and *p*ATP was weak and that it was difficult to form a monolayer directly on the Ge surface. On the other hand, it is more likely that electrons given by Ge favor passing through the Ag-NPs to reduce the silver ions to form the second layer of Ag-NPs.

To examine the impact of the initial layer on the formed second layer of Ag-NPs, substrates of 30^1AgS and 50^1AgS were also re-grown in 0.5 mM of silver nitrate solution for different lengths of time. The resulting band intensities of *p*ATP obtained with these substrates are also plotted in Fig. 3B. As can be seen in this figure, the signals increased as the re-growing time increased, but approached a maximal value around a re-growing time of 20 minutes, for any of the substrates. To observe the newly formed Ag-NPs after re-growing in silver nitrate, substrates of 30^1AgS/$25^{0.5}$Ag and 50^1AgS/$25^{0.5}$Ag were scanned by SEM; the resulting images are plotted in Figs. 4G and 4H. They show that the morphologies were similar to those indicated by the images of 10^1AgS/$25^{0.5}$Ag (Fig. 4F). However, the images also show a denser distribution of the Ag-NPs and their corresponding signals were higher than that of 10^1AgS/$25^{0.5}$Ag as shown in Fig. 3B.

Effect of the Concentration of Silver Nitrate on the Second Layer of Silver Nanoparticles. To examine the effect of the concentration of silver nitrate on growing the second layer of Ag-NPs, solutions of silver nitrate in concentrations of 0.3 to 1.0 mM were used to grow the second layer of Ag-NPs on substrates of 10^1AgS and 30^1AgS. The resulting changes in the band intensities of the *p*ATP are plotted against the re-growing time for different concentrations of silver nitrate, as shown in Figs. 5A and 5B for substrates of 10^1AgS and 30^1AgS, respectively. As can be seen from Fig. 5A, there is an optimal signal for each concentration of $AgNO_3$ examined. Based on the maximum signals, the morphologies of the Ag-NPs prepared under the optimal conditions for different concentrations of $AgNO_3$ should be slightly different. At long reaction times, the Ag-NPs that were formed tended to percolate, leading to increased band distortion. Those conditions at which distortion was particularly severe are indicated by the open symbols in Fig. 5A. Percolation of the Ag-NPs began at a reaction time of about 35, 25, and 20 minutes for 0.5, 0.7, and 1 mM $AgNO_3$ solutions, respectively. A similar conclusion can be drawn for the 30^1AgS substrate re-grown in different concentrations of silver nitrate; the resulting maxi-

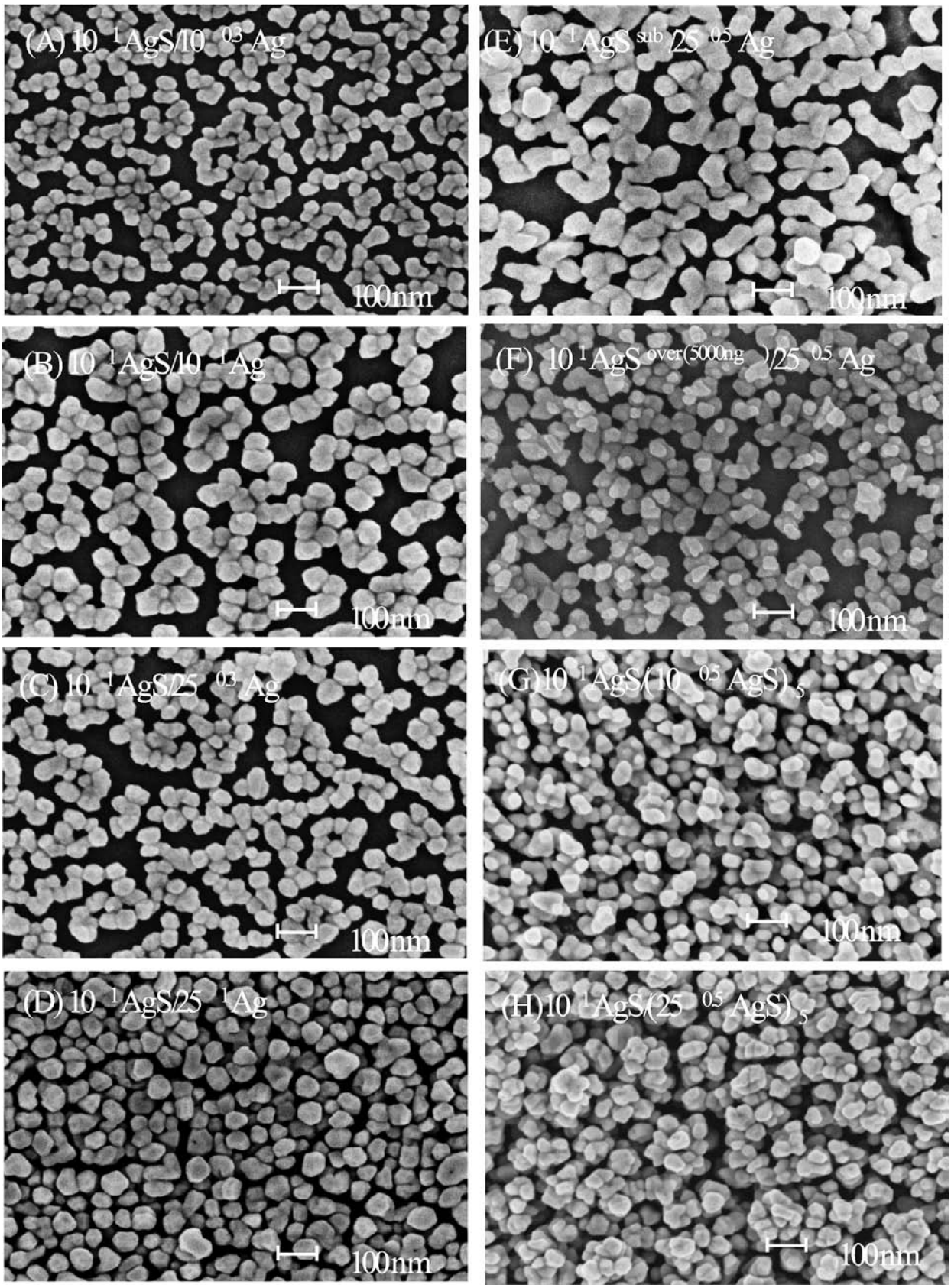

FIG. 6. SEM images of (**A**) $10^{1}AgS/10^{0.3}Ag$, (**B**) $10^{1}AgS/10^{1}Ag$, (**C**) $10^{1}AgS/25^{0.3}Ag$, (**D**) $10^{1}AgS/25^{1}Ag$, (**E**) $10^{1}AgS^{sub}/25^{0.5}Ag$, (**F**) $10^{1}AgS^{over(5000ng)}/25^{0.5}Ag$, (**G**) $10^{1}AgS/(10^{0.5}AgS)_5$, and (**H**) $10^{1}AgS/(25^{0.5}AgS)_5$.

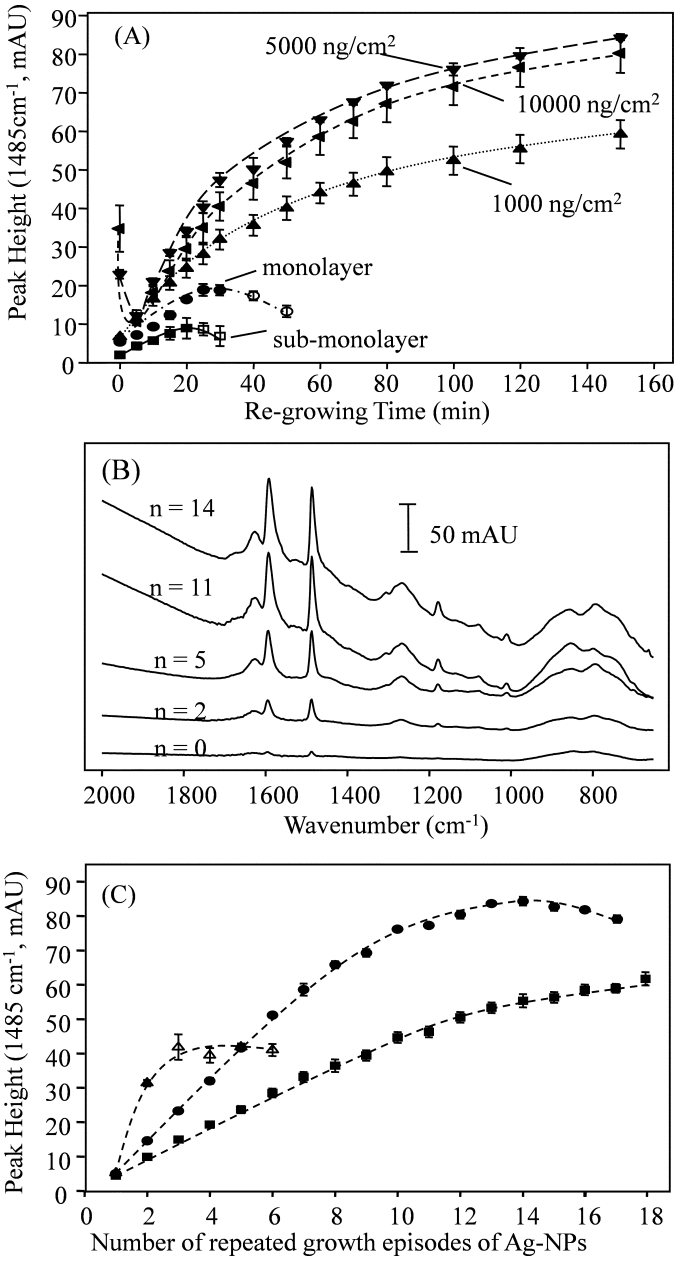

FIG. 7. (**A**) Band intensities of *p*ATP observed on 10^1AgS after re-growing in 0.5 mM silver nitrate solution for different reaction times. *p*ATP was varied to have a coverage fraction of 50% sub-monolayer (■), monolayer (●), and over-layers (monolayer with a further deposition of 1000 (▲), 5000 (▼), and 10000 ng/cm^2 (◀) of *p*ATP). Distortion of the band shape was observed as labeled by the open symbols. (**B**) Spectra of *p*ATP on substrates of 10^1AgS/($10^{0.5}$AgS)n, where $n = 0$, 2, 5, 11, and 14. (**C**) Relationship between band intensities of *p*ATP and number of re-growing times. The re-growing times were controlled for 5 (■), 10 (●), and 25 (▲) minutes. Distortion of the band shape was observed as labeled by the open symbols.

mum signals differed slightly with varying concentrations of silver nitrates, as can be seen in Fig. 5B.

To observe any significant differences between the Ag-NPs re-grown in different concentrations of silver nitrate, the morphologies of substrates of 10^1AgS/$10^{0.3}$Ag and 10^1AgS/$10^{1.0}$Ag were examined by SEM; the resulting images are shown in Figs. 6A and 6B. The substrates of 10^1AgS/$25^{0.3}$Ag and 10^1AgS/$25^{1.0}$Ag were also examined and the results are shown in Figs. 6C and 6D. Based on Fig. 5A, with a re-growing time of 10 minutes, none of the resulting spectra showed distorted bands. Their corresponding SEMs, shown in Figs. 6A and 6B, indicate that particles are well separated, but that the higher the silver concentration, the larger the size of the formed particles when the reaction time is held constant. Based on these images and the signals in Fig. 5A, a particle size of 100 nm, as shown in Fig. 6B, produces a larger signal in SEIRA measurements. For a reaction time of 25 minutes, the resulting bands of *p*ATP were derivative-shaped for re-growing solutions of silver nitrate in concentrations higher than 0.7 mM as shown in Fig. 5A. The images in Figs. 6C and 6D for substrates prepared in a re-growing time of 25 min illustrate that the degree of non-isolated particles is increased as the concentration is increased.

Effect of the Coverage of *p*-Aminothiophenol on Silver Nanoparticles in Re-growing of Silver Nanoparticles. To examine the influence of the density of the *p*ATP monolayer on the re-grown Ag-NPs, experiments were designed to vary the amount of *p*ATP on the Ag-NPs, from less than a monolayer (under-layer), to a monolayer, to an over-layer of molecules. Substrates of 10^1AgS were used and the concentration of silver nitrate for re-growing of Ag-NPs was a consistent 0.5 mM for all the reactions. To form a full monolayer of coverage, the substrates were soaked in *p*ATP solution for a minimum of 20 hours. Compared to the signals from direct deposition, the Ag-NPs with the monolayer of coverage were estimated to have a surface density of 160 ng/cm^2. To produce sub-monolayers of *p*ATP, substrates were soaked in *p*ATP solution for 30 minutes. By comparing the resulting signals to the signals of monolayer, the surface density was obtained as around 80 ng/cm^2, which represents a coverage of 50% of the surface of the Ag-NPs. To form an over-layer, a monolayer of *p*ATP was formed, followed by deposition of different amounts of *p*ATP. The signals observed for different re-growth times in silver nitrate solution are plotted in Fig. 7A. SEM images of Ag-NPs with the sub-monolayer and over-layer of coverage (5000 ng/cm^2) for re-growing are shown in Figs. 6E and 6F, respectively. As can be seen in Fig. 7A, the signals of substrates with the sub-monolayer of coverage increased slightly compared to the signals of the substrates before re-growing of Ag-NPs. As Fig. 6E shows, the growing of Ag-NPs for an insufficient coverage is similar to the formation of the first layer Ag-NPs as SEM shows in Fig. 4B. When larger quantities of *p*ATP were deposited on the monolayer-covered Ag-NPs, further re-growing of Ag-NPs yielded the intense bands seen in Fig. 7A. The observed signals for an over-layer of coverage were decreased in the first few minutes of reaction time. This behavior can be explained by the solubility of the deposited *p*ATP in aqueous solution, such that a portion of the un-reacted *p*ATP dissolved in the water, causing the signals to decrease. Then, after the second layer of Ag-NPs began to form, the enhancement effect occurred, leading to a subsequent increase of the detected signals. The SEM image in Fig. 6F shows that the Ag-NPs can form even when the first layer of Ag-NPs is completely covered by *p*ATP, revealing that electrons from Ge can still pass through the coverage layer to the silver ions in the bulk solution. Compared to the SEM in Fig. 4F for mono-layer coverage with 25 min of re-growing time, the particle size formed with an over-layer of coverage under the same conditions was much smaller.

Behavior in Repeating the Growing Procedures. To examine the performance when the substrates were subjected to

repeated episodes of Ag-NP growth, substrates of 10^1AgS were used to repeatedly grow Ag-NPs at constant re-growing times of either 10 minutes or 25 minutes. Figures 7B and 7C show typical spectra and the relationship between the number of times of repeated re-growth and the band intensities. Corresponding SEM images are shown in Figs. 6G and 6H. The IR spectra indicate that the Ag-NPs were isolated with no derivative-shaped bands. The Ag-NPs produced by repeating the growing procedure were round in shape and several layers thick, as indicated by the images in Figs. 6G and 6H, indicating that multiple layers of isolated Ag-NPs can be grown on Ge substrates through the new surface modification method.

CONCLUSION

In this work, a growing procedure was demonstrated to produce round-shaped Ag-NPs whose size can be controlled to optimize the SEIRA signals. When a second layer of Ag-NPs was formed on a pre-grown layer of Ag-NPs, the observed signals for *p*ATP between the two layers showed an increase of two to five times. Based on SEM photos, the newly formed Ag-NPs were round in shape and showed much higher density in distribution than the initial layer of Ag-NPs. The observed SEIRA spectra did not exhibit derivative-shaped bands for *p*ATP on the Ag-NPs after re-growth, indicating that *p*ATP was sandwiched between the layers of Ag-NPs, preventing direct contact between the two layers of Ag-NPs. The reaction conditions can be fine-tuned to vary the morphology and thickness of the Ag-NPs. Also, by repeating the growing procedures, a thick layer of stacked Ag-NPs with sizes optimized for SEIRA measurements can be obtained readily and could be highly suitable for chemical sensing applications.

ACKNOWLEDGMENT

The authors thank the National Science Council of the Republic of China for their financial support of this work.

1. A. Hartstein, J. R. Kirtley, and J. C. Tsang, Phys. Rev. Lett. **45,** 201 (1980).
2. E. A. Coronado and G. C. Schatz, J. Chem. Phys. **119,** 3926 (2003).
3. M. Osawa, K. I. Ataka, K. Yoshii, and Y. Nishikawa, Appl. Spectrosc. **47,** 1497 (1993).
4. G. Q. Lu, S. G. Sun, L. R. Cai, S. P. Chen, and Z. W. Tian, Langmuir **16,** 778 (2000).
5. D. A. Heaps and P. R. Griffiths, Vib. Spectrosc. **42,** 45 (2006).
6. Y. Nakao and H. Yamada, Surf. Sci. **176,** 578 (1986).
7. Y. Nishikawa, K. Fujiwara, and T. Shima, Appl. Spectrosc. **44,** 691 (1990).
8. Y. Nishikawa, K. Fujiwara, and T. Shima, Appl. Spectrosc. **45,** 747 (1991).
9. Y. Nishikawa, Y. Ito, K. Fujiwara, and T. Shima, Appl. Spectrosc. **45,** 752 (1991).
10. M. Osawa and M. Ikeda, J. Phys. Chem. **95,** 9914 (1991).
11. J. Yang and P. R. Griffiths, Anal. Bioanal. Chem. **388,** 109 (2007).
12. R. Kellner, B. Mizaikoff, M. Jakusch, H. D. Wanzenbock, and N. Weissenbacher, Appl. Spectrosc. **51,** 495 (1997).
13. G. T. Merklin and P. R. Griffiths, J. Phys. Chem. B **101,** 5810 (1997).
14. G. T. Merklin and P. R. Griffiths, Langmuir **13,** 6159 (1997).
15. H. D. Wanzenbock, B. Mizaikoff, N. Weissenbacher, and R. Kellner, J. Mol. Struct. **410,** 535 (1997).
16. S. Geng, J. Friedrich, J. Gahde, and L. Guo, J. Appl. Polym. Sci. **71,** 1231 (1999).
17. M. Osawa, K. I. Ataka, M. Ikeda, H. Uchihara, and R. Nanba, Anal. Sci. **7,** 503 (1991).
18. A. E. Bjerke and P. R. Griffiths, Anal. Chem. **71,** 1967 (1999).
19. R. Aroca and B. Price, J. Phys. Chem. B **101,** 6537 (1997).
20. F. Hahn and C. A. Melendres, Electrochim. Acta **46,** 3525 (2001).
21. M. S. Zheng, S. G. Sun, and S. P. Chen, J. Appl. Electrochem. **31,** 749 (2001).
22. M. S. Anderson, Appl. Phys. Lett. **83,** 2964 (2003).
23. J. Zhang, J. Zhao, H. He, H. Zhang, H. Li, and Z. Liu, Langmuir **14,** 5521 (1998).
24. S. Sanchez-Cortes, C. Domingo, J. V. Garcia-Ramos, and J. A. Aznarez, Langmuir **17,** 1157 (2001).
25. J. Yang and S. H. Chen, Appl. Spectrosc. **55,** 399 (2001).
26. L. A. Porter, H. C. Choi, A. E. Ribbe, and J. M. Buriak, Nano. Lett. **2,** 1067 (2002).
27. A. Rodes, J. M. Orts, J. M. Perez, J. M. Feliu, and A. Aldaz, Electrochem. Commun. **5,** 56 (2003).
28. L. Magagnin, R. Maboudian, and C. Carraro, J. Phys. Chem. B **106,** 401 (2002).
29. C. Carraro, L. Magagnin, and R. Maboudian, Electrochim. Acta **47,** 2583 (2002).
30. H. Miyake, S. Ye, and M. Osawa, Electrochem. Commun. **4,** 973 (2002).
31. S.-J. Huo, X.-K. Xue, Q.-X. Li, S.-F. Xu, and W.-B. Cai, J. Phys. Chem. B **110,** 25721 (2006).
32. Y.-G. Yan, Q.-X. Li, S.-J. Huo, M. Ma, W.-B. Cai, and M. Osawa, J. Phys. Chem. B **109,** 7900 (2005).
33. A. Miki, S. Ye, and M. Osawa, Chem. Commun. 1500 (2002).
34. Q.-X. Li, X.-K. Xue, Q.-J. Xu, and W.-B. Cai, Appl. Spectrosc. **61,** 1328 (2007).
35. B.-B. Huang, J.-Y. Wang, S.-J. Huo, and W.B. Cai, Surf. Interface Anal. **40,** 81 (2008).
36. H. Miyake and M. Osawa, Chem. Lett. **33,** 278 (2004).
37. H.-F. Wang, Y.-G. Yan, S.-J. Huo, W.-B. Cai, Q.-J. Xu, and M. Osawa, Electrochemica Acta, **52,** 5950 (2007).
38. H. Miyake, E. Hosono, M. Osawa, and T. Okada, Chem. Pheys. Lett. **428,** 451 (2006).